WORLD CONFERENCE ON TIMBER ENGINEERING 2025
BRISBANE, AUSTRALIA
Advancing Timber for the Future Built Environment

# TIMBER FAILURE AT SCREW TIPS ON GLULAM REINFORCED BY SELF-TAPPING SCREWS

Junki Tateyama[1], Daisuke Kanagaki[2], Marina Totsuka[3]*, Takeo Hirashima[4]

**ABSTRACT:** This paper investigates timber compressive failure at screw tips on glulam beams reinforced by self-tapping screws. The timber failure at the screw tips has high ductility and a gradual load increase after yielding. However, this failure mode occurred less frequently than other modes, and a prediction of the timber failure at the screw tips was mismatched with experimental values in previous studies. To correctly assess the bearing capacity of the timber failure at the screw tips, we conducted experiments with 9 and 36 specimens for central and corner column-beam joints, respectively. For the central column-beam joints, the timber failure at the screw tips occurred with 18 screws but not 12 screws. For the corner column-beam joints, the timber failure at the screw tips occurred in all specimens reinforced by screws. Therefore, the timber failure at the screw tips hardly occurs in the central column-beam joints and often occurs in the corner column-beam joints. Stress spreading in the corner column-beam joints differed from that in the central ones. Moreover, the bearing capacity of the timber failure at the screw tips was less affected by screw lengths and increased with an arrangement of more screws farther from an edge.

**KEYWORDS:** compression perpendicular to grain, glulam beams, column-beam joints, reinforcement, self-tapping screws

## 1 – INTRODUCTION

Recently, developments of high-strength and high-stiffness joints have become prevalent due to an expanding utilization of timber structures for medium to large-scale buildings. At column-beam joints in the timber structures, a bearing strength and stiffness perpendicular to the grain are often dominant [1]. Consequently, increasing the bearing strength and stiffness perpendicular to the grain is essential for achieving the high-strength and high-stiffness joints.

One method for enhancing the bearing capacity and stiffness is reinforcement by self-tapping screws like piles in a loaded area on beams [2-4]. Bejtka et al. investigated the failure mechanisms of the timber beams reinforced by self-tapping screws [5]. In their study, three failure modes were observed: pushing-in failure, buckling failure, and timber failure at the screw tips. Previous studies have accurately evaluated the bearing capacity for the pushing-in and buckling failures [6]. The timber failure at the screw tips occurs when the timber at the screw tips reaches compressive strength perpendicular to the grain. Therefore, the strength of the timber failure at the screw tips depends on the effective length [$l_{ef,2}$] (in Fig. 1) of the compressive area formed in the screw tips. In the model of Karlsruhe, the effective length [$l_{ef,2}$] is calculated by assuming that an angle of stress spreading is 45 degrees [7]. However, it has been suggested that there is a gap between the predicted and experimental values [8-9].

In order to correctly predict the effective length [$l_{ef,2}$], we conducted an experimental study on specimens in two load conditions estimating central and corner column-beam joints.

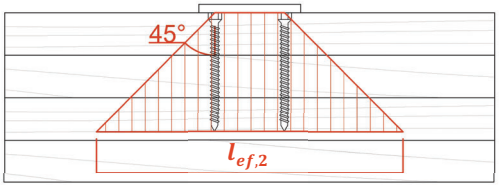


*Figure 1. Effective length for the timber failure at the screw tips*

[1] Junki Tateyama, Graduate School of Engineering and Science, Chiba University

[2] Daisuke Kanagaki, Graduate School of Engineering and Science, Chiba University

[3] Corresponding author, Marina Totsuka, Graduate School of Engineering, Chiba University, Chiba, Japan, 263-8522, ORCID 0000-0001-8548-4996

[4] Takeo Hirashima, Graduate School of Engineering, Chiba University


https://doi.org/10.52202/080513-0679

## 2 – MATERIALS AND METHODS

Table 1 shows an overview of the specimens. For the central column-beam joints, the specimens were homogeneous glulam of Japanese cedar (*Cryptomeria japonica,* E65-F255 according to the JAS [10]) with an average moisture content (MC) of 8.1 % and average density of 360 kg/m$^3$. The dimensions were 1500 mm × 120 mm × 300 mm (length × width × height). The test variables were the number of screws (12 or 18) and the penetration length of the screws (140, 200 or 260 mm). Material tests were conducted for compression perpendicular to the grain according to EN408 [11]. The

*Table 1. Overview of specimens and test results*

| Series | Center or corner | Screw | | | Specimen length [mm] | Load case | Samples | Compressive strength by material test [N/mm$^2$] | Experimental result | | |
|---|---|---|---|---|---|---|---|---|---|---|---|
| | | Arrangement | Number | Length [mm] | | | | | Bearing capacity [kN] (Ave.) | $l_{ef,2}$ [mm] | $l_{ef,3}$ [mm] |
| C4-3-140 | Center | 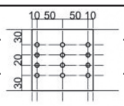 | 12 | 140 | 1500 | A | 1 | 2.35 | 191.3 | | |
| C4-3-200 | Center | | 12 | 200 | 1500 | A | 1 | 2.35 | 230.1 | | |
| C4-3-260 | Center | | 12 | 260 | 1500 | A | 1 | 2.35 | 284.8 | | |
| C4-3-140-3×2 | Center | 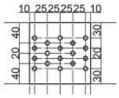 | 18 | 140 | 1500 | A | 2 | 2.35 | 196.1 | | |
| C4-3-200-3×2 | Center | | 18 | 200 | 1500 | A | 2 | 2.35 | 279.5 | | |
| C4-3-260-3×2 | Center | | 18 | 260 | 1500 | A | 2 | 2.35 | 308.0 | | |
| C0K | Corner | — | — | — | 600 | A | 3 | 2.04 | 45.5 | — | — |
| C0DK | Corner | — | — | — | 600 | B | 3 | 2.04 | 43.4 | — | — |
| C2-2-140K | Corner | 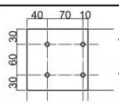 | 4 | 140 | 600 | A | 3 | 2.04 | 70.9 | 290 | 180 |
| C2-2-140DK | Corner | | 4(8) | 140 | 600 | B | 3 | 2.04 | 80.2 | 328 | 218 |
| C2-2-260K | Corner | | 4 | 260 | 600 | A | 3 | 2.04 | 75.7 | 309 | 199 |
| C2-1-260K | Corner | 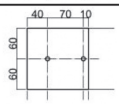 | 2 | 260 | 600 | A | 3 | 2.04 | 72.8 | 297 | 187 |
| C2-4-260K | Corner | 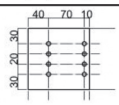 | 8 | 260 | 600 | A | 3 | 2.04 | 83.1 | 339 | 229 |
| C2-2-260KB | Corner | 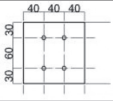 | 4 | 260 | 600 | A | 3 | 3.39 | 92.2 | 227 | 147 |
| C2-2-260KUB | Corner | 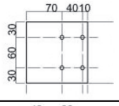 | 4 | 260 | 600 | A | 3 | 3.39 | 119.4 | 294 | 184 |
| C1-2-260KS | Corner | 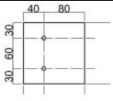 | 2 | 260 | 600 | A | 3 | 3.39 | 73.4 | 181 | 141 |
| C1-2-260KE | Corner | 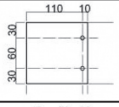 | 2 | 260 | 600 | A | 3 | 3.39 | 103.1 | 254 | 144 |
| C2-2-140DKL | Corner | 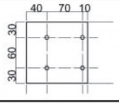 | 4(8) | 140 | 990 | B | 3 | 3.39 | 110.5 | 272 | 162 |

Note: *Total number of screws on the upper side; the symbol "()" indicates the total on the upper and lower sides.

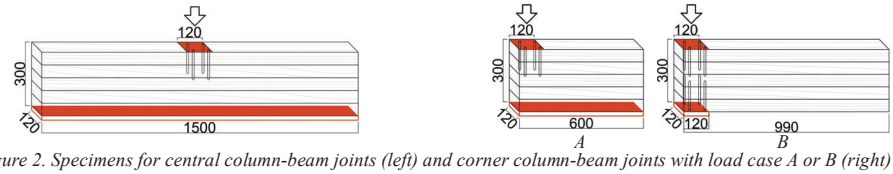


*Figure 2. Specimens for central column-beam joints (left) and corner column-beam joints with load case A or B (right)*

https://doi.org/10.52202/080513-0679

six samples' average compressive strength and Young's modulus were 2.35 N/mm$^2$ and 281 N/mm$^2$, respectively.

For the corner column-beam joints, seven series of the specimens (C0K, C0DK, C2-2-140K, C2-2-140DK, C2-2-260K, C2-1-260K and C2-4-260K) were homogeneous glulam of Japanese cedar (*Cryptomeria japonica*, E65-F255 according to the JAS [10]) with average MC of 10.5 % and average density of 371 kg/m$^3$. The dimensions were 600 mm × 120 mm × 300 mm. The test variables were the number of screws (0, 2, 4, or 8), penetration length of the screws (140 or 260 mm), and loading conditions (cases A and B in Fig. 2). Case A shows a specimen with the reinforced area on the upper side supported by a foundation on the lower side. Case B shows a specimen with reinforced areas on both sides, and in this case, the support on the lower side matches the size of the loaded area. The six samples' average compressive strength and Young's modulus were 2.04 N/mm$^2$ and 216 N/mm$^2$, respectively. The remaining five series of specimens (C2-2-260KB, C2-2-260KUB, C1-2-260KS, C1-2-260KE and C2-2-260DKL) for the corner column-beam joints were homogeneous glulam of Japanese cedar (*Cryptomeria japonica*, E65-F255 according to the JAS [10]) with average MC of 8.3 % and average density of 402 kg/m$^3$. The dimensions were 600 or 990 mm × 120 mm × 300 mm. The test variables were screw arrangement and specimen lengths. The six samples' average compressive strength and Young's modulus were 3.39 N/mm$^2$ and 216 N/mm$^2$, respectively.

A diameter of the screws was 8 mm for both column-beam joints. All specimens with screw reinforcement were pre-drilled with a diameter of 5 mm in a length of approximately 100 mm by using an impact driver. The screws were drilled at a right angle, and the head of the screw was flushed with the timber surface in all specimens.

## 3 – EXPERIMENTAL SETUP

Fig. 3 shows the experimental setup. A compressive load was motorically displacement-controlled through the steel plate; a deformation rate was 2 mm/min, the load area was 120 mm × 120 mm, and loads were ended when a displacement at the steel plate exceeded 20 mm or 30 mm. For each specimen, the displacement of the steel plate was measured at two points, and the average was used in subsequent discussions and the deformation rate. In addition, a digital image correlation (DIC) system using a digital camera (XOS, Canon) and a DIC software (GOM Correlate, GOM) were employed to analyze surface strains in one sample per series as shown in Fig. 4. The images were captured at a frequency of 0.2 Hz during the test. A speckle pattern was created using matte white paint and black lacquer spray.

## 4 – RESULTS

A maximum load was taken as the bearing capacity for the specimens with a definite maximum load. Otherwise, the bearing capacity was calculated according to EN408 [11]. Table 1 lists the bearing capacities.

### 4.1 LOAD-DISPLACEMENT RELATIONSHIPS AND FAILURE MODES

Figs. 5-9 show the failure modes. The pushing-in failure was a combination of the pushing-in failure of the screws and the failure occurring at the timber contact surface (Fig. 5). The buckling failure was characterized by the buckling of the screws in the timber and the failure at the timber contact surface (Fig. 6). The timber failure at the screw tips was characterized by the compression of the timber at the screw tips. An expansion of the timber near the screw tips was observed (Fig. 7).

Fig. 10 shows the load-displacement relationship for the central column-beam joints, and Fig. 11 shows the load-displacement relationship for the corner column-beam joints.

For the central column-beam joints, the specimen with 12 screws showed the pushing-in failure regardless of the penetration length of the screws. The load-displacement relationship is dependent on the penetration length of the screws. For the specimen with 140 mm screws, after reaching the maximum load, the load continued to decrease slowly. For the specimens with 200 mm screws and 260 mm screws, the load was reduced by 20-30% after reaching the maximum load. After the load dropped, it increased slightly but then dropped slowly again. The specimen with 18 screws yielded due to the timber failure at the screw tips and then reached the maximum load due to the pushing-in failure regardless of the penetration length of the screws. After reaching the maximum load, the load decreased or decreased temporarily and remained stable.

For the corner column-beam joints, all specimens reinforced by screws yielded due to the timber failure at the screw tips. After yielding, the pushing-in or buckling failure occurred in some specimens. The load continued to increase slowly after the timber failure at the screw tips and decreased after the pushing-in and buckling failure. In some specimens, the load was temporarily reduced after maximum load due to a cracking failure (Fig. 8) or


https://doi.org/10.52202/080513-0679

a bending failure (Fig. 9) of the timber. For the non-reinforced specimens (C0K and C0DK), the load increased slowly after yielding. In C2-4-260K, the displacement reached 20-30 mm before reaching the maximum load capacity, and the load continued to grow until unloading.

It can be considered that the timber failure at the screw tips is unlikely to occur for the central column-beam joints but is quite likely to occur for the corner column-beam joints.

## 4.2 STRAIN DISTRIBUTION ON SPECIMEN SURFACE BY DIC

Fig. 12 shows the vertical strain distribution on the specimen surface at 80% of the maximum load by the DIC for the central column-beam joints. Fig. 13 shows the vertical strain distribution on the specimen surface at the bearing capacity by the DIC for the corner column-beam joints.

For the central column-beam joints, the lines in Fig. 12 show angles from the screw heads: black line represents 45 degrees and red line 60 degrees. From the surface strain distribution, it can be seen that the stress spreads at a certain angle. The angle is constant regardless of the penetration length of the screws and is more significant than 60 degrees (red line in Fig. 12) in the specimen with the timber failure at the screw tips (C4-3-140-3×2, C4-3-200-3×2, and C4-3-260-3×2).

For the corner column-beam joints, it can be seen that the compressive stresses do not spread at the certain angle unlike the case of the central column-beam joints. The compressive strain of C2-2-260KUB was more spread than that of C2-2-260KB, and the compressive strain of C1-2-260KE was more spread than that of C1-2-260KS. This indicates that the compressive stress spreads as the number of the screws farther from the edge increases. Comparing C2-2-140DK with C2-2-140DKL, there was no difference in the compressive strain distribution, suggesting that the length of the specimen does not affect

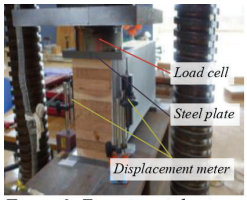

Figure 3. Experimental setup.

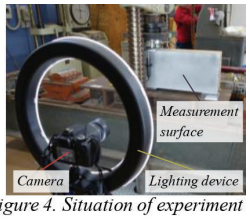

Figure 4. Situation of experiment with digital imaging correlation.


Figure 5. Pushing-in failure.

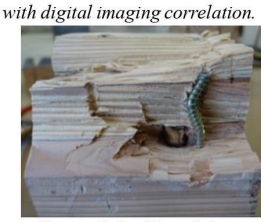
Figure 6. Buckling failure.


Figure 7. Timber failure.


Figure 8. Cracking failure.

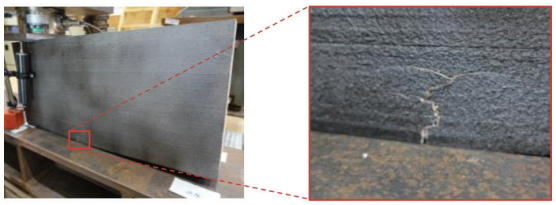
Figure 9. Bending failure.

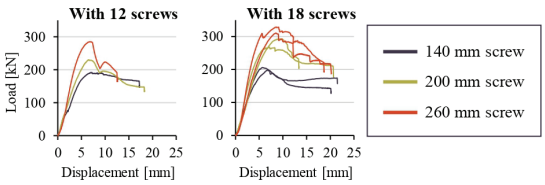

Figure 10. Load-displacement relationships for central column-beam joints.

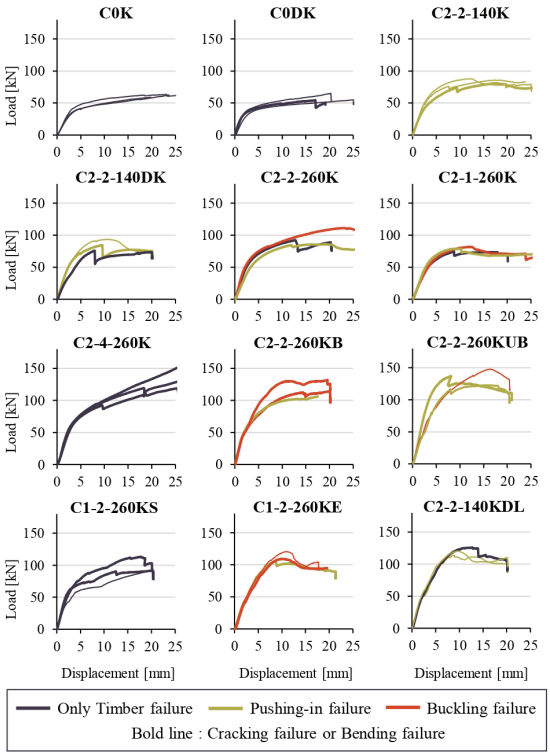

Figure 11. Load-displacement relationships for corner column-beam joints.

https://doi.org/10.52202/080513-0679

the compressive stress distribution. Therefore, the 600 mm length provided a sufficient margin.

## 4.3 COMPARISON OF BEARING CAPACITY BY TEST VARIABLES

Figs. 14 and 15 show comparisons of the different variables (number of screws, penetration length of screws, load case, and screw arrangement), including the results from the previous study [6].

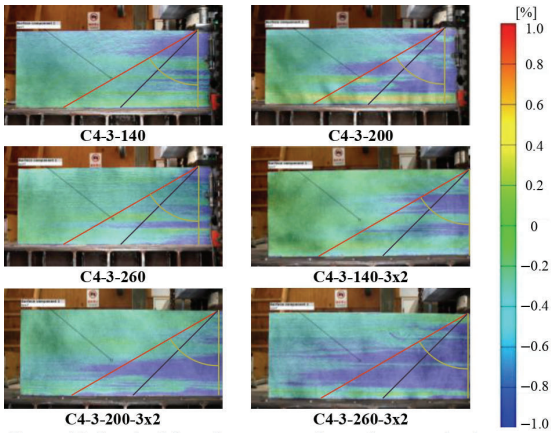


*Figure 12. Result of digital image correlation for central column-beam joints*

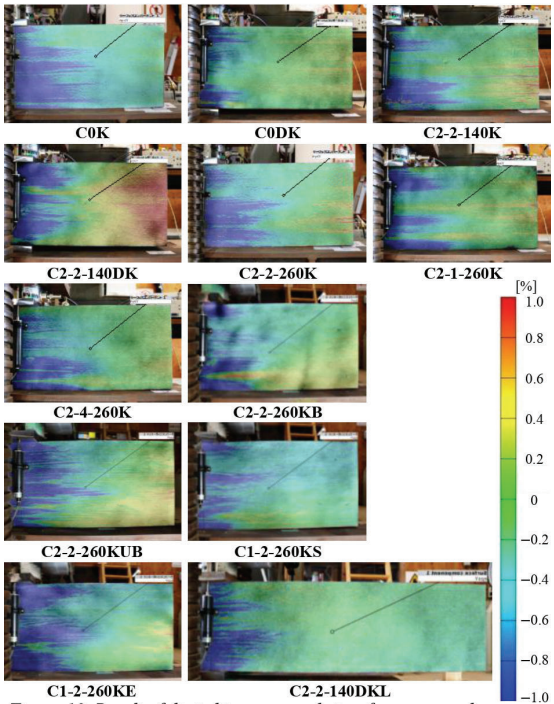


*Figure 13. Result of digital image correlation for corner column-beam joints*

### 4.3.1 Penetration length of screws

For the central column-beam joints, when using 4 and 12 screws, the bearing capacity increased in proportion to the penetration length of the screws. When using 18 screws, the bearing capacity increased as the penetration length of the screw increased, but the rate of the increase tended to converge. This was not the case with 4 or 12 screws, suggesting that there is no upper limit to the effect of increasing penetration length of the screws and that the decrease in effect with 18 screws may be due to the spacing between the screws.

For the corner column-beam joints, the bearing capacity of C2-2-260K was 1.07 times that of C2-2-140K. The strain distribution by the DIC (Fig. 13) showed that the stress state did not change with the penetration length of the screws. Therefore, it is considered that the effective length [ $l_{ef,2}$ ] (in Fig. 16) is independent of the penetration length of the screws.

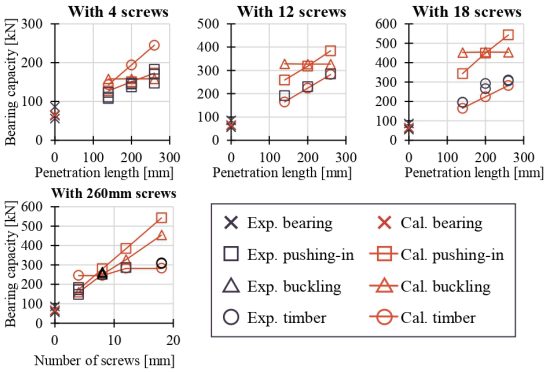


*Figure 14. Comparison of bearing capacity by test variables and comparison between predictions and experimental results for central column-beam joints.*

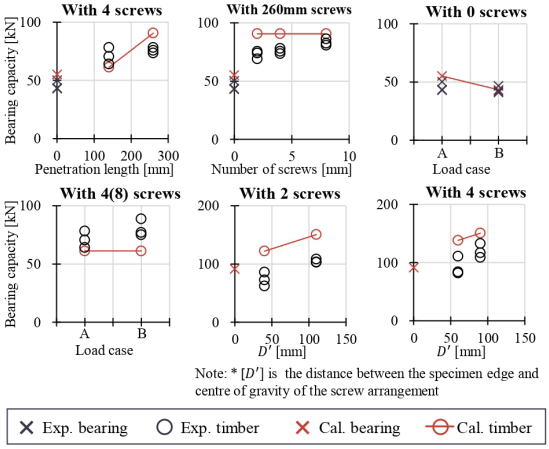


*Figure 15. Comparison of bearing capacity by test variables and comparison between predictions and experimental results for corner column-beam joints.*


https://doi.org/10.52202/080513-0679

### 4.3.2 Number of screws

For the central column-beam joints, the effect of the number of screws on the bearing capacity was significant with the increase from 0 to 8 screws. After that (i.e. 12 and 18 screws), the increase in bearing capacity was less marked. The pushing-in and the buckling failure occurred in specimens with 4 to 12 screws, and the timber failure at the screw tips occurred in specimens with 18 screws. It is considered that the change in the failure mode with the increase in the screw number affected the increase in the bearing capacity. In addition, the fact that the effect converges after the 8 screws are used suggests that there may be an upper limit to the effect of increasing the screw number on the bearing capacity.

For the corner column-beam joints, the C0K, C2-1-260K, C2-2-260K and C2-4-260K series were compared. The bearing capacity of C2-1-260, C2-2-260K, and C2-4-260K was 1.60, 1.66, and 1.83 times that of C0K, respectively. There was a significant difference between the specimens with and without the screw reinforcement. However, the increase in screw number from 2 to 8 was moderate, suggesting that the effect of the screw number was small.

### 4.3.3 Load case (for corner column-beam joints)

The bearing capacity of C2-2-140K was 1.56 times that of C0K. The bearing capacity of C2-2-140DK was 1.85 times greater than that of C0DK. The screw reinforcement in load case B had a more significant effect on the bearing capacity than that in load case A.

### 4.3.4 Screw arrangement (for corner column-beam joints)

The bearing capacity of C2-2-260KUB was 1.30 times greater than that of C2-2-260KB, and that of C1-2-260KE was 1.40 times greater than that of C1-2-260KS. This suggests that the bearing capacity increases as the screw placement is farther from the specimen edge.

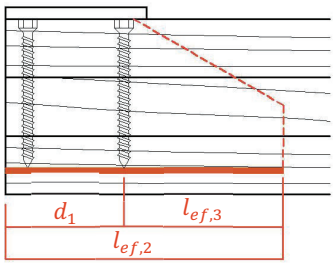


*Figure 16. Effective length for corner column-beam joints*

## 5 – COMPARISON BETWEEN PREDICTIONS AND EXPERIMENTAL RESULTS

For the central column-beam joints, Fig. 14 compares the predictions using the proposed formula [6] and the experimental results of the bearing capacity. First, the bearing capacity of the timber failure at the screw tips was compared. The predictions were slightly smaller than the experimental values (0.76 ~ 0.92 times the experimental values). Second, the bearing capacity of the pushing-in failure was compared. The predictions were larger than the experimental values (1.35～1.38 times). Therefore, the following (1) was used to calculate the experimental value of the bearing capacity per screw, $R_{d,exp}$, calculated from the experimental bearing capacity. $R_{d,exp}$ was then compared to the predicted capacity per screw in the case of the pushing-in failure calculated using (2).

$$R_{d,exp} = \frac{R_{90,d,exp} - R_{d,0}}{n} \quad (1)$$

$R_{d,exp}$ : Bearing capacity per screw (experimental value)
$R_{90,d,exp}$ : Bearing capacity (experimental value)
$R_{d,0}$ : Bearing capacity (experimental value of non-reinforced specimens of previous study)
$n$ : Number of screws

$$R_{d,cal} = 0.6 \cdot \sqrt{d} \cdot {l_s}^{0.9} \cdot \rho^{0.8} \quad (2)$$

$R_{d,cal}$ : Bearing capacity per screw (predicted value)
$d$ : Diameter of screw
$l_s$ : Penetration length of screw
$\rho$ : Density of wood

As a result, the predictions for the specimen with the pushing-in failure were 1.48 to 1.59 times higher than the experimental values, indicating an overestimation. The previous study (4-8 screws) showed that the $R_{d,cal}$ values were concordant with the experimental values, ranging from 0.97 to 1.14 times [6]. However, the comparison in the present report shows a large difference between the predictions and the experimental results. This may be attributed to the distance between the screws being insufficient in the present experiment.

For the corner column-beam joints, Fig. 15 compares the predictions using the proposed formula [7] and the experimental results of the bearing capacity. The bearing

https://doi.org/10.52202/080513-0679

capacity of the timber failure at the screw tips was compared. The predictions varied significantly from the experimental values (0.69 to 1.96 times), suggesting that the capacity model stresses spread at 45 degrees is incorrect. Therefore, a capacity model different from that for the central column-beam joints is necessary.

## 6 – EFFECTIVE LENGTH

For the central column-beam joints, experimental values for the angle of stress spread (in Fig. 1) related to the effective length of the plane formed at the tip of the screws, $l_{ef,2}$, were calculated from the following (3).

$$\alpha_{exp} = \tan^{-1}\left[\left\{\left(R_{90,d,exp}/bf_{c,90,d} - l_{ss}\right)/2\right\}/l_s\right] \quad (3)$$

$\alpha_{exp}$ : Angle of stress spread (experimental value)

$l_s$ : Penetration length of the screws

$R_{90,d,exp}$ : Bearing capacity (experimental value)

$b$ : Width of specimen

$f_{c,90,d}$ : Compressive strength perpendicular to the grain

$l_{ss}$ : Distance between screws

The resulting experimental angle of the stress spread was an average of 64.3 degrees. Therefore, when calculating the predicted bearing capacity of the timber failure at the screw tips, the angle of the stress spread can be calculated at 60 degrees for safety reasons.

For the corner column-beam joints, the experimental values for the effective length of the plane formed at the tip of the screws, $l_{ef,2}$, were calculated from the following (4) and shown in Table 1.

$$l_{ef,2} = R_{90,d,exp}/(b \cdot f_{c,90,d}) \quad (4)$$

The results suggest that the effective length, $l_{ef,2}$, depends on the position of the screw farthest from the specimen edge. Therefore, the effective length, $l_{ef,3}$, is defined as shown in Fig. 16 and calculated using (5) and shown in Table 1.

$$l_{ef,3} = R_{90,d,exp}/(b \cdot f_{c,90,d}) - d_1 \quad (5)$$

$d_1$ : Distance from the edge of the specimen to the farthest screw

From C2-2-260KB and C2-2-260KUB, when there are four screws, $l_{ef,3}$ is considered to be larger when the screw arrangement is farther from the specimen edge. From C1-2-260KS and C1-2-260KE, it is considered that $l_{ef,3}$ does not change depending on the screw arrangement when there are two screws. From C2-2-260KUB and C1-2-260KE, $l_{ef,3}$ is considered to increase with the inclusion of screws on the edge side of the specimen. Also, $l_{ef,3}$ increases slightly with an increase in the number of screws. Based on the above, Fig. 17 shows three graphs of the specimen with load case A, where the vertical axis is $l_{ef,3}$ and the horizontal axis is $[D']$, [N], and $[D'] \times$ [N], respectively. $[D']$ is the distance between the specimen edge and the center of gravity of the screw arrangement. [N] is the number of the screws. Since the specimens for the corner column-beam joints in this study were made of two batches of the timber with different material properties, each specimen was examined separately. As a result, a strong positive correlation was found between $l_{ef,3}$ and $[D'] \times$ [N].

## 7 – EFFICIENCY OF A SCREW GROUP

For the central column-beam joints, a comparison presented in Section 5 confirms that the predictions and the experimental values for the bearing capacity per screw in the pushing-in failure do not match. The efficiency of a screw group (all the screws on one specimen) decreases with the number of the screws in the same area. The relationship between the bearing capacity per screw and $A_{s,exp}$ is investigated in this paper. $A_{s,exp}$ in this paper is the applied force area (120 mm × 120 mm) divided by the number of screws. In Fig. 18, $R_{d,exp}$ (used in the calculations in Section 5) is on the vertical axis and $A_{s,exp}$ on the horizontal axis. Equation (1) was also used to calculate $R_{d,exp}$ for specimens with the timber failure at the screw tips.

For specimens with a screw penetration length of 260 mm, when $A_{s,exp}$ decreases below 1800 mm$^2$, $R_{d,exp}$

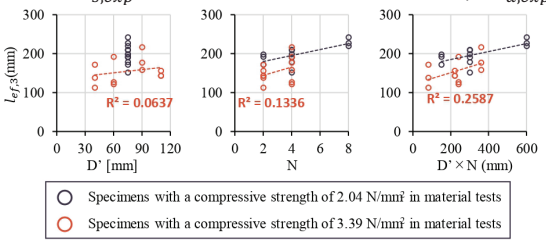


*Figure 17. Relationship between $l_{ef,3}$ and* D', N or D' × N

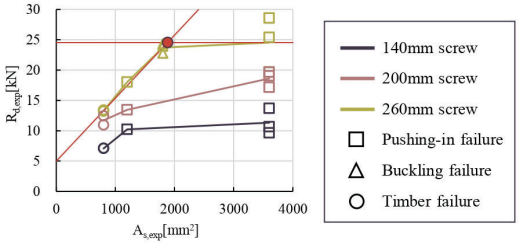


*Figure 18.* $R_{d,exp}$ - $A_{s,exp}$ *relationship for central column-beam joints.*


https://doi.org/10.52202/080513-0679

decreases rapidly. The failure mode of the specimens also changes with a decrease in $A_{s,exp}$, with the failure due to screws (buckling and pushing-in) above 1800 mm$^2$ and the timber failure at the screw tips at 800 mm$^2$. This suggests that the failure due to screws and the timber failure at the screw tips may occur in the section between 800 mm$^2$ and 1800 mm$^2$. The intersection of the bearing capacity at 3500 mm$^2$ and the extension of the straight line from 800 mm$^2$ to 1800 mm$^2$ (red point in Fig. 18) is approximately 1900 mm$^2$, suggesting that this point may be a boundary point where the decrease in $R_{d,exp}$ occurs. In the future, a more detailed investigation of the value of $A_{s,exp}$ will be conducted by obtaining data in the interval from 1800 mm$^2$ to 3500 mm$^2$.

## 8 – CONCLUSION

We conducted the experimental study on the specimens to investigate the behavior and correctly predict the bearing capacity of the timber compressive failure at screw tips on glulam beams reinforced by self-tapping screws.

The timber failure at the screw tips is unlikely to occur for the central column-beam joints but is quite likely to occur for the corner column-beam joints.

For the central column-beam joints, the stress spreads at the certain angle from the loading plate. The experimental angle was 64.3 degrees. For safety reasons, the prediction with the angle of 60 degrees is recommended. From the examination of the relationship between the bearing capacity per screw $R_{d,exp}$ and the applied force area per one screw $A_{s,exp}$, $R_{d,exp}$ decreased as $A_{s,exp}$ became smaller. In addition, $R_{d,exp}$ significantly decreased when $A_{s,exp}$ was below a certain point. This indicates that the load-bearing capacity per screw may decrease when the screw spacing is narrow. Future studies should consider the effects of screw spacing for practical applications.

For the corner column-beam joints, the maximum reinforcement effect was 1.83 times (compared to the non-reinforced specimen), which was lower than that for the central column-beam joints. The mechanism of the timber failure at the screw tips, especially the compressive stress spreading in the specimens, was different from that for the central column-beam joints. Therefore, a new evaluation method was proposed. The bearing capacity was affected by the distance between the specimen edge and the center of gravity of the screw arrangement $[D']$ and the number of the screws [N], and there was a strong correlation between the bearing capacity and $[D'] \times$ [N]. Therefore, it is considered that more screws farther from the specimen edge are effective.

## 9 – REFERENCES


[1] A. J. M. Leijten. “The bearing strength capacity perpendicular to grain of norway spruce − Evaluation of three structural timber design models.” Construction and Building Materials 105 (2015), pp.528-535

[2] P. Dietsch, R. Brandner. “Self-tapping screws and threaded rods as reinforcement for structural timber elements-a state-of-the-art report.” Construction and Building Materials 97 (2015), pp.78–89.

[3] H.J. Blaß, P. Schädle. “Ductility aspects of reinforced and non-reinforced timber joints.” Engineering Structures 33 (2011), pp.3018-3026

[4] A. Aloisio, E. Ussher, M. Fragiacomo et al. “Capacity models for timber under compression perpendicular to grain with screw reinforcement” Eur. J. Wood Prod 81 (2023), pp.633–654.

[5] I. Bejtka “Verstärkung von Bauteilen aus Holz mit Vollgewindeschrauben.” PhD thesis. Universitätsverlag Karlsruhe – Versuchsanstalt für Stahl, Holz und Steine (VAKA), 2005.

[6] D. Kanagaki et al. “Reinforcement for compression perpendicular to grain in column-base and -beam joints using partially threaded and fully threaded screws” Engineering Structures 324 (2025), 119334

[7] I.Bejtka et al. “Self-Tapping Screws as Reinforcements in Beam Supports.” CIB-W18 (2006), 39-7-2

[8] A. Aloisio et al “Buckling capacity model for timber screws loaded in compression: Experimental, analytical and FE investigations.” Construction and Building Materials 379 (2023), 131225

[9] R. Tomasi et al. “Experimental investigation on screw reinforcement of timber members under compression perpendicular to the grain.” Engineering Structures 275 (2023), 115163

[10] JAS 1152, Japanese Agricultural Standard, Glued Laminated Timber, 2023.

[11] EN408:2010+A1:2012